Optogenetic activation of septal cholinergic neurons suppresses sharp wave ripples and enhances theta oscillations in the hippocampus

Marie Vandecasteele[a,b], Viktor Varga[a,c], Antal Berényi[a,d,e], Edit Papp[c], Péter Barthó[c], Laurent Venance[b], Tamás F. Freund[c], and György Buzsáki[a,d,1]

[a]Center for Molecular and Behavioral Neuroscience, Rutgers University, Newark, NJ 07102; [b]Center for Interdisciplinary Research in Biology, Institut National de la Santé et de la Recherche Médicale U1050, Centre National de la Recherche Scientifique, Unité Mixte de Recherche 7241, Collège de France, F-75005 Paris, France; [c]Institute of Experimental Medicine, Hungarian Academy of Sciences, H-1083, Budapest, Hungary; [d]Neuroscience Institute, School of Medicine, New York University, New York, NY 10016; and [e]MTA-SZTE "Momentum" Oscillatory Neuronal Networks Research Group, Department of Physiology, University of Szeged, H-6720, Szeged, Hungary

Edited by Ranulfo Romo, Universidad Nacional Autonóma de México, Mexico City, D.F., Mexico, and approved August 5, 2014 (received for review June 25, 2014)

Theta oscillations in the limbic system depend on the integrity of the medial septum. The different populations of medial septal neurons (cholinergic and GABAergic) are assumed to affect different aspects of theta oscillations. Using optogenetic stimulation of cholinergic neurons in ChAT-Cre mice, we investigated their effects on hippocampal local field potentials in both anesthetized and behaving mice. Cholinergic stimulation completely blocked sharp wave ripples and strongly suppressed the power of both slow oscillations (0.5–2 Hz in anesthetized, 0.5–4 Hz in behaving animals) and supratheta (6–10 Hz in anesthetized, 10–25 Hz in behaving animals) bands. The same stimulation robustly increased both the power and coherence of theta oscillations (2–6 Hz) in urethane-anesthetized mice. In behaving mice, cholinergic stimulation was less effective in the theta (4–10 Hz) band yet it also increased the ratio of theta/slow oscillation and theta coherence. The effects on gamma oscillations largely mirrored those of theta. These findings show that medial septal cholinergic activation can both enhance theta rhythm and suppress peri-theta frequency bands, allowing theta oscillations to dominate.

acetylcholine | channelrhodopsin-2 | silicon probe | in vivo electrophysiology

Subcortical neuromodulators play a critical role in shifting states of the brain (1, 2). State changes can occur both during sleep and in the waking animal and are instrumental in affecting local circuit computation that supports various functions, including attention, learning, memory, and action (3–5). The septo-hippocampal cholinergic system has been hypothesized to play a critical role in setting network states in the limbic system (4, 6). ACh can affect both short- and long-term plasticity of synaptic connections and provide favorable conditions for encoding information (7–9). These plastic states are associated with hippocampal theta oscillations (10). High theta states are characterized by increased release of ACh that varies in a task-dependent manner on the time scale of seconds (11–13). In contrast, reduced cholinergic activity allows effective spread of excitation in the recurrent CA3 network, giving rise to synchronous sharp wave ripples (SPW-R) (14–16).

Inactivation of the medial septum (MS)/diagonal band of Broca abolishes theta oscillations in the hippocampus and entorhinal cortex (17) and results in severe learning deficit (18, 19). Similarly, selective toxin lesion of septal cholinergic neurons produces a several-fold decrease of theta power but not its frequency (20). The phase of the local field potentials (LFP) theta oscillations shifts from the septal to the temporal pole and in the CA3–CA1 axis by ∼180° (21, 22). Thus, at each point in time neurons residing at different locations of the three-dimensional structure of the hippocampus spike at different theta phases yet are bound together by the global theta signal. These numerous sources of theta generators are believed to be coordinated by the reciprocal connections between the septum and hippocampus (23), but the nature of this spatial–temporal coordination is not well understood (24). Both cholinergic and GABAergic neurons, and a small fraction of VGlut2 immunoreactive neurons (25), are believed to play a critical role in such global coordination (26, 27). Although GABAergic neurons of the MS were demonstrated to be entrained at theta frequency, identified cholinergic neurons did not show theta-related discharge pattern (28, 29). Additionally, both GABAergic and cholinergic neurons are affected by the feedback long-range hippocampo-septal inhibitory connections (30).

Early studies, performed in anesthetized animals, already suggested a critical role for the cholinergic septo-hippocampal projection in the generation of theta oscillations (6). Indeed, the low-frequency theta present under urethane anesthesia can be fully abolished by antimuscarinic drugs (31). In contrast, atropine or scopolamine fail to abolish theta oscillations during waking exploration (31, 32), although they affect the theta waveform and its amplitude-phase depth profile in the hippocampus (33). Although these previous works are compatible with the hypothesis that the role of septal cholinergic projections is mainly permissive and affects theta power without modulating its frequency (20, 26, 28), direct evidence is missing. The role of septal cholinergic neurons on gamma oscillation and SPW-R is even less understood (14). To address these issues, we used optogenetic activation of septal cholinergic input and examined its impact on hippocampal theta, peri-theta bands, gamma, and ripple oscillations in both anesthetized and freely moving mice.

Significance

Theta oscillations are a prominent rhythm of the brain occurring during active behavior and rapid eye movement sleep and thought to provide the temporal frame for the encoding of information. Acetylcholine modulation is a major player in hippocampal theta rhythm, as demonstrated by lesion and pharmacological manipulations of cholinergic receptors, yet the link between the activity of septal cholinergic neurons and the theta rhythm is not fully understood. We used specific optogenetic stimulation of the septo-hippocampal cholinergic neurons in the anesthetized and behaving mouse to decipher the effects of cholinergic stimulation on hippocampal network activity and show that in addition to promoting theta oscillations it suppresses sharp wave ripples and peri-theta band activity.

Author contributions: M.V., V.V., and G.B. designed research; M.V., V.V., A.B., and E.P. performed research; L.V. and T.F.F. contributed new reagents/analytic tools; P.B., L.V., and T.F.F. provided a physiology setup; M.V., V.V., E.P., and P.B. analyzed data; and M.V., V.V., and G.B. wrote the paper.

The authors declare no conflict of interest.

This article is a PNAS Direct Submission.

[1]To whom correspondence should be addressed. Email: Gyorgy.Buzsaki@nyumc.org.

This article contains supporting information online at www.pnas.org/lookup/suppl/doi:10.1073/pnas.1411233111/-/DCSupplemental.

Results

To address the role of the septo-hippocampal cholinergic input, we used mice expressing light-activated cation channel channelrhodopsin-2 tagged with a fluorescent protein (ChR2-YFP) under the control of the choline-acetyl transferase promoter (ChAT). These mice displayed an intense YFP-positive staining in MS ChAT neurons, as shown by double immunostaining in transgenic hybrid (Fig. 1*A*) and virus-injected mice (Fig. S1*A*) and YFP- and ChAT-positive fibers in the target structures of the MS, including the hippocampus (Fig. S1*B*).

Light-Responsive Cells in the Medial Septum. First, using urethane-anesthetized mice, we verified that illumination of the MS induced a light-entrained activity of putative ChAT neurons. To this end, we constructed optrodes by placing an etched and sharpened optic fiber (diameter <10 μm) glued on the shank(s) of a multisite silicon probe (34). Brief pulses of light (10–100 ms) were applied at 0.5 Hz continuously while the optrode was descended into the MS (Fig. S1*C*), until responsive units were identified. Responsive neurons reliably followed trains of pulses (Fig. 1*C1*) and sine stimulations between 0.5 and 12 Hz (Fig. 1*D*), whereas at frequencies >10 Hz spike adaptation was observed (Fig. 1*C2*). All light-responsive cells (n = 6 cells from n = 4 mice) had slow spontaneous firing rates (median firing rate 0.57 Hz, range 0.04–1.9 Hz). Half of the driven cells significantly increased their firing frequency in response to a tail pinch although they stayed within a slow-firing range (<4 Hz; Fig. 1*B*), consistent with the typical activity of cholinergic neurons (28, 29).

Hippocampal Responses to MS Stimulation. Whereas cholinergic neurons faithfully followed the frequency of stimulation, the frequency of theta oscillation in the hippocampus was not affected (Fig. 1*E*). To ensure that this effect was not due to the low intensity of light delivered by the optrode (<0.6 mW at the tip), in subsequent experiments a multimode optic fiber (50- to 105-μm core, yielding 5–10 mW maximal light intensity) was implanted in the MS and multisite, linear silicon probes were used to record hippocampal activity in anesthetized and freely moving mice.

Suppression of hippocampal sharp wave ripples. The most prominent and consistent effect of optogenetic stimulation of MS cholinergic neurons was the suppression of SPW-Rs recorded in the CA1 pyramidal layer (Fig. 2). Ripple occurrence was significantly suppressed or abolished during MS stimulation (1–12 Hz, sine stimulation or pulse trains, 1–60 s) in mice recorded either during urethane anesthesia (n = 6 mice, median suppression –90%, P = 0.0312) or during free behavior (n = 8, median suppression –92%, P < 0.01). The few surviving SPW-Rs during the stimulation were similar to ripples detected in control epochs (Fig. S2). The effective suppression of SPW-Rs demonstrated that MS stimulation exerted a physiological impact on the operations of hippocampal circuits in both anesthetized and behaving mice.

Effect on hippocampal LFP power. MS stimulation had an apparently differential effect on theta oscillations in anesthetized and behaving mice. Whereas under both conditions MS stimulation reduced the power in the slow (0.5–2 Hz in anesthetized, 0.5–4 Hz in behaving animals) and supratheta bands (6–10 Hz in anesthetized, 10–25 Hz in behaving animals), it increased theta power in anesthetized mice but it decreased or had no effect on theta power in behaving mice (Fig. 3).

Under anesthesia, stimulation of the MS typically switched hippocampal activity from large-amplitude, irregular activity (35) to a theta state (Fig. 3*A*). Spectral analysis of 10-s-long stimulation segments relative to 10-s control segments before stimulation (Fig. 3 *B* and *C*) showed that the MS stimulation effect was most prominent at lower frequencies (<30 Hz). Optogenetic stimulation induced a strong increase of power at 3–4 Hz ("urethane theta," ref. 31), whereas both lower (0.5–2 Hz) and upper (6–10 Hz) neighboring frequency bands were strongly decreased. The impact on theta was most prominent in stratum lacunosum-moleculare (LM, Fig. 3*C*). Across animals, the effect on theta power increase was significant individually in six of seven anesthetized mice (2–6 Hz; group median change +1.5 dB, $P < 10^{-21}$, n = 296 trials; Fig. S3*A*). Stimulation also significantly decreased power in the slow oscillation band (0.5–2 Hz; –3.5 dB, $P < 10^{-31}$) and in the supratheta band (6–10 Hz; –0.9 dB, $P < 10^{-11}$). Optogenetic stimulation in the MS of ChAT-cre mice injected by a virus carrying only the fluorescent reporter enhanced YFP (EYFP) induced no detectable changes in hippocampal activity (Fig. S4).

The theta/slow oscillation ratio increased in six out of seven anesthetized mice (group: +207%, $P < 10^{-33}$). To further analyze

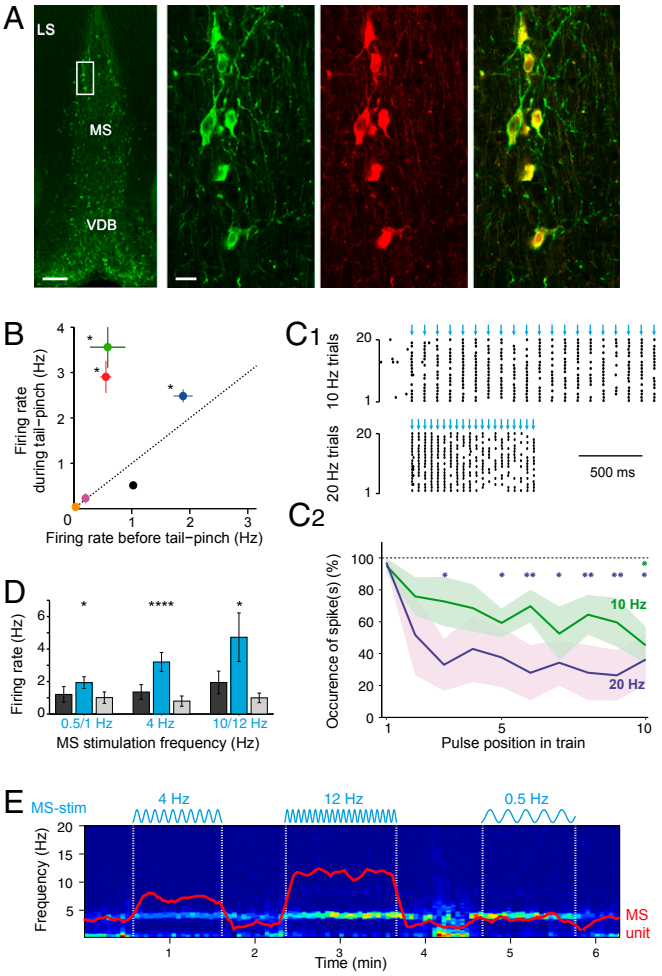

Fig. 1. Entrainment of MS neurons by blue light stimulation. (*A*) Left-most panel: YFP-positive immunostaining in a coronal section of the MS in a ChAT-ChR2-YFP hybrid transgenic mouse. LS, lateral septum; VDB, ventral diagonal band. (Scale bar: 200 μm.) Right panels: higher magnification of the MS (rectangle in left panel), double immunostaining of YFP (green, left), and ChAT (red, middle), showing their perfect colocalization (overlay, right; 100% overlap in n = 108 and n = 111 neurons in two mice). (Scale bar: 10 μm.) (*B*) Spontaneous activity of all light-entrained cells. Asterisks indicate a significant difference in the mean firing rate in response to tail pinch (mean ± SEM, n = 4 trials, paired t test). (*C1*). Raster plot activity of an entrained cell in response to 10 Hz (*Upper*) and 20 Hz (*Lower*) trains of optogenetic stimulations (15-ms pulses, blue arrows). (*C2*) The reliability of spiking decreases at higher frequencies (mean ± SEM, n = 4 neurons). Asterisks indicate a significantly lower spike occurrence compared with the first pulse (repeated-measures ANOVA with Bonferroni post-hoc test). (*D*) Mean firing rates of MS entrained cells in response to sinusoidal stimulations. Asterisks indicate significant differences between control and stimulation epochs (n = 5 cells tested during spontaneous and tail pinch-evoked activity, repeated-measures ANOVA with Bonferroni post-hoc test). (*E*) Spectrogram of hippocampal LFP in LM during sine stimulation of the MS. Red: mean firing rate of a simultaneously recorded MS unit (same y axis scale as the spectrogram). *P < 0.05, **P < 0.01, ***P < 0.001, ****$P < 10^{-4}$.

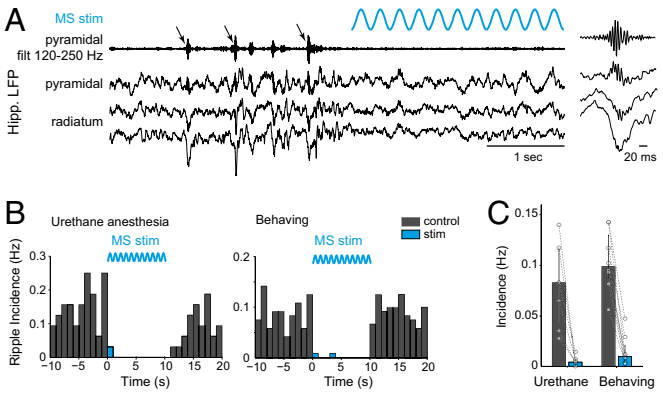

Fig. 2. MS stimulation suppresses hippocampal sharp wave ripples. (*A*) Example of hippocampal LFP in the pyramidal layer and stratum radiatum displaying SPW-R (arrows) before the onset of optogenetic stimulation. (*Inset*) Magnification of a detected ripple. (*B*) Peristimulus time histogram of ripple occurrence, before, during, and after 10-s sine stimulations at 1–12 Hz, recorded in the same mouse under urethane anesthesia (*Left*, $n = 77$ trials) or during free behavior (*Right*, $n = 128$ trials). (*C*) The mean incidence of ripples is significantly decreased during stimulation in both urethane anesthesia ($n = 6$ mice) and freely moving conditions ($n = 8$ mice). Bars/error bars, medians and quartiles for all animals; paired dots, individual mice.

this effect at a finer timescale, we used wavelet decomposition to identify theta epochs within each control and stimulation epoch: Each sample was classified as theta-dominated if the scale corresponding to the maximal coefficient of the wavelet decomposition fell into theta band (2–6 Hz for anesthesia). We found that the proportion of theta-dominated samples per epoch was significantly increased by optogenetic stimulation of MS cholinergic neurons in all mice (median proportion increase +0.33, $P < 10^{-32}$, $n = 296$ trials; $n = 7$ mice, range: +0.08 to +0.64; see also Fig. S5).

In waking, freely moving mice, MS stimulation significantly decreased the power in the slow oscillation (0.5–4 Hz; −1.5 dB, $P < 10^{-18}$) and supratheta (10–25 Hz; −1.6 dB, $P < 10^{-38}$) bands (Fig. 3 *B* and *C*). In contrast to that in anesthetized mice, theta power (4–10 Hz) in waking, freely moving mice was moderately but significantly decreased (median change −0.8 dB, $P < 10^{-28}$, $n = 417$ trials, $n = 4$ mice, range −0.2 to −1.4 dB). However, the theta/slow oscillation ratio increased significantly (median: +15%, $P = 0.0024$). In addition, the median proportion of theta-dominated samples per epoch increased from 0.30 in control to 0.43 in stimulation epochs ($P < 10^{-7}$; see also Fig. S5). Therefore, even though theta power was decreased, the stronger effect on peri-theta bands concurred to increase relative theta prominence in the LFP.

In two mice, recordings were performed in both anesthetized and behaving conditions (example in Fig. 3*B*). Changes in these mice reflected the group effects presented above and further demonstrated the differential effect of cholinergic stimulation on theta oscillation between anesthetized and drug-free animals.

Cholinergic activation effects on gamma-band oscillations were largely similar to those on theta-band oscillations, albeit with lower magnitude. Under anesthesia, the slow gamma oscillations (<40 Hz) increased in multiple layers, whereas gamma power (both slow, 30–70 Hz and midgamma, 70–100 Hz) decreased in waking animals (Fig. S6 *A*–*C*). Theta phase modulation of gamma power was not altered by optogenetic stimulation (Fig. S6*D*).

Effect on hippocampal LFP coherence. The theta-promoting effect of MS stimulation was further confirmed by coherence analysis across hippocampal layers (Fig. 4). In particular, stratum radiatum (Rad)-LM coherence increased at 3–4 Hz during stimulation under anesthesia and in the 2- to 7-Hz band in behaving animals [Fig. 4*A* and Fig. S3*B*; median change in theta band: +0.09 in anesthetized animals (2–6 Hz), $P < 10^{-25}$, individually significant in six of seven animals; +0.06 in behaving animals (4–10 Hz), individually significant in four of four mice]. The MS stimulation-induced coherence increase in theta band under anesthesia (2–6 Hz) was significant across all layer pairs, whereas in the behaving animal (4–10 Hz) it was confined to Rad–LM and oriens–pyramidal layer pairs (Fig. 4*B*). The induced coherence increase in behaving animals was restricted to frequencies below 7 Hz, indicating that cholinergic activation of the hippocampus selectively affected the slow form of theta oscillations (31). The induced power and coherence changes of the LFP described above were largely confirmed by analyzing spectral changes of current source density signals as well (Fig. S7).

To examine the impact of the frequency of MS stimulation, we compared trials with 1-, 4-, 8-, and 12-Hz trains. In no experiment did we observe that the frequency of the hippocampal LFP followed the frequency of MS stimulation (Fig. 1*E* and Fig. S8). In several cases, increasing the frequency of stimulation increased the magnitude of power changes (Fig. S8). This effect is likely due to the fact that faster stimulation induced more spikes and therefore higher levels of ACh released from the cholinergic terminals in the hippocampus (36).

State dependence of MS stimulation effect. Visual inspection of the LFP traces indicated that the relative magnitude of the MS stimulation-induced effects depended on background hippocampal activity. Because the strongest effect was the suppression

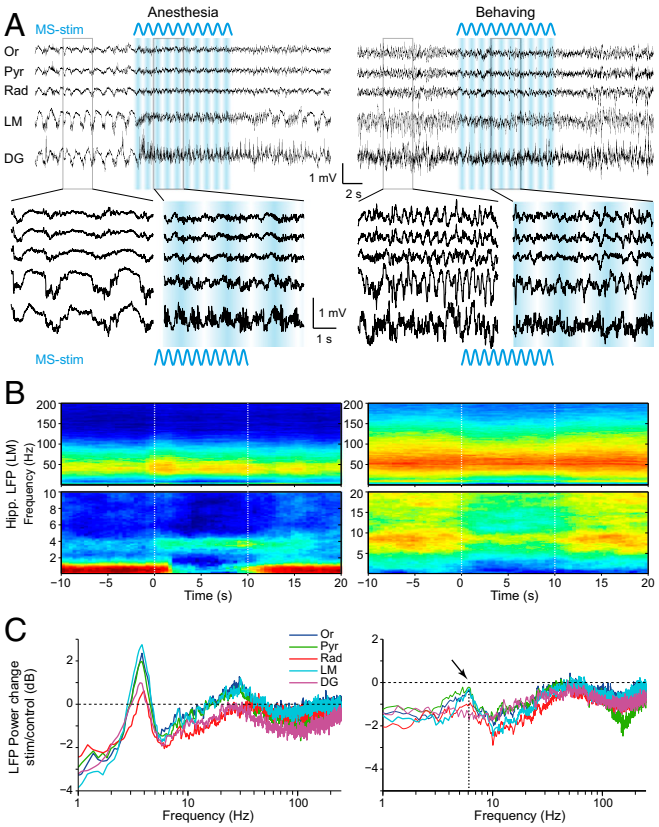

Fig. 3. MS stimulation exerts a selective effect at theta and peri-theta frequencies in both anesthetized (*Left*) and behaving (*Right*) mouse. (*A*) Example of hippocampal LFP from five layers. Blue: MS sinusoidal stimulation. (*Lower*) magnified view of 3 s from control and stimulation epochs. (*B*) Spectrograms of LFP recorded in LM in the same mouse under both conditions before, during, and after 10-s sine stimulation (median of $n = 71$ trials in anesthesia, $n = 82$ in behaving). LFP was whitened for better visualization of higher frequencies. (*Lower*) Zoom on lower frequencies. (C) LFP power change in hippocampal layers (median of all trials, $n = 296$ in seven anesthetized mice, $n = 417$ in four behaving mice). Arrow and dotted line indicates the spared (least suppressed) frequency (~6 Hz). DG, dentate gyrus; LM, stratum lacunosum-moleculare; Or, stratum oriens; Pyr, pyramidal layer; Rad, stratum radiatum.

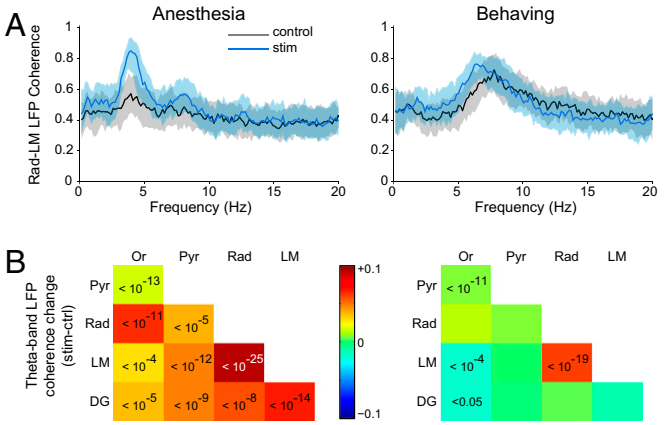

Fig. 4. MS stimulation promotes hippocampal theta coherence. (*A*) Rad-LM coherence spectrum in control (black) and stimulation (blue) epochs in representative animals (median ± quartiles of all trials, $n = 98$ in anesthesia, $n = 82$ in behaving). (*B*) MS stimulation-induced coherence change for theta band (anesthesia: 2–6 Hz, behaving: 4–10 Hz). For each layer pair, the color indicates the median change (all trials pooled), and significant *P* values are indicated (Wilcoxon's rank sum test with Bonferroni's correction for 10 layer pairs).

of SPW-Rs, we segregated trials into two groups: those displaying at least one ripple event during the control period (10 s preceding the onset of stimulation, "ripple trials") and those without ripples and with a dominant power in the theta band ("theta-dominant trials"). Because theta and SPW-Rs do not rapidly alternate (37), the presence of SPW-Rs in the prestimulation epochs can be taken as an indication of a different overall state compared with epochs with prominent theta oscillations. In anesthetized animals, LFP power in LM showed a larger relative effect of stimulation in ripple trials than in theta-dominant trials (Fig. 5 *A* and *B*; theta/slow oscillation ratio in ripple trials: +402%, $P < 10^{-11}$, $n = 69$ trials vs. theta-dominant trials: +155%, $P < 10^{-6}$, $n = 84$ trials). The differential effect of stimulation was also apparent in the changes of dominant frequency. In ripple trials, the median frequency shifted from a slow-oscillation range to theta band (from 1.1 to 3.8 Hz, $P < 10^{-10}$), whereas stimulation did not affect the median frequency in theta-dominant trials (3.7 Hz in both control and stimulation epochs; $P > 0.1$; Fig. 5*B*).

MS stimulation also exerted a background state-dependent differential effect in behaving mice. In ripple trials, MS stimulation induced a global decrease in LFP power with a relative sparing at ~6 Hz, resulting in a moderate but significant increase in the theta/slow oscillation ratio (Fig. 5 *C* and *D*; +27%; $P < 10^{-11}$, $n = 165$ trials) and also increased theta proportion during the stimulation epoch (Fig. 5*D*). The dominant frequency increased significantly from 3.8 Hz to 6 Hz during stimulation ($P = 0.0012$; Fig. 5*D*). In contrast, during theta-dominant trials the theta/slow oscillation ratio and the proportion of theta samples were not significantly changed, and theta frequency was significantly decreased (from 7.3 Hz to 6.9 Hz, $P < 10^{-3}$). The power in the supratheta (10–25 Hz) band was significantly reduced in both ripple (−47%, $P < 10^{-23}$) and theta-dominant (−21%, $P < 10^{-11}$) trials.

It may be argued that SPW-Rs events are more likely followed by theta epochs and, conversely, epochs with high theta power may be more likely followed by epochs with low theta power. To control for such potential sampling bias, we compared pairs of consecutive 10-s epochs of spontaneous activity in the same way as control vs. stimulation epoch pairs were analyzed. Epochs were pseudorandomly chosen by shifting the analyzed epochs by −20 s (i.e., comparing a "pre" interval located −30 to −20 s before stimulation onset to a "post" interval located −20 to −10 s before the stimulation onset). The lack of significant changes in these control analyses confirmed the validity of our statistical analyses of the MS-induced effects (Fig. S9). In summary, optogenetic activation of MS cholinergic neurons was more effective in the absence of background theta activity. When background epochs were already dominated by high theta power, MS stimulation induced only moderate or no effects.

Behavioral Effects of MS Stimulation. To assess the behavioral correlates of the physiological effects observed on hippocampal activity, we measured locomotor activity on a linear track or in an open field in three behaving mice equipped with movement-tracking light-emitting diodes during stimulation (Fig. 6). Considering the dichotomy of the MS stimulation effect depending on background LFP activity (discussed in *State dependence of MS stimulation effect*), we similarly segregated LFP epochs into ripple trials vs. theta-dominant trials. During ripple trials, associated with lower locomotor activity, MS stimulation significantly increased speed in two of the three mice. In contrast, in theta-dominant trials, speed was decreased significantly during stimulation compared with control epochs in two of the three mice. Therefore, the dichotomous effects on behavior were consistent with the effects on theta power described above. The correlations between locomotion speed and theta power and speed and theta frequency were preserved during MS stimulation (Fig. 6*C*). These findings indicate that optogenetic cholinergic activation did not alter the relationship between theta and behavior.

Discussion

Optogenetic stimulation of the cholinergic septal neurons induced theta and gamma oscillations in the urethane-anesthetized mouse. However, in waking, exploring mice the impact of stimulation on theta and gamma oscillations was less expressed and largely masked by the faster, noncholinergic form of theta. The strongest effects of cholinergic stimulation were observed on abolishing SPW-Rs and reducing the power of slow and supratheta oscillations under both anesthesia and waking state. Thus, a main effect of ACh in theta oscillations seems to be the reduction of competing nontheta mechanisms.

The most consistent effect of optogenetic activation of septal cholinergic neurons was the suppression of SPW-Rs (Fig. 2). Because such an effect was observed in every session in both anesthetized and waking animals, SPW-R suppression most clearly illustrates the effectiveness of optogenetic stimulation. These findings support the hypothesis that SPW-Rs are initiated by the excitatory recurrent collaterals of CA3 pyramidal neurons when subcortical controlling neuromodulatory transmitters are reduced (14). ACh may attenuate the spread of such excitation by reducing

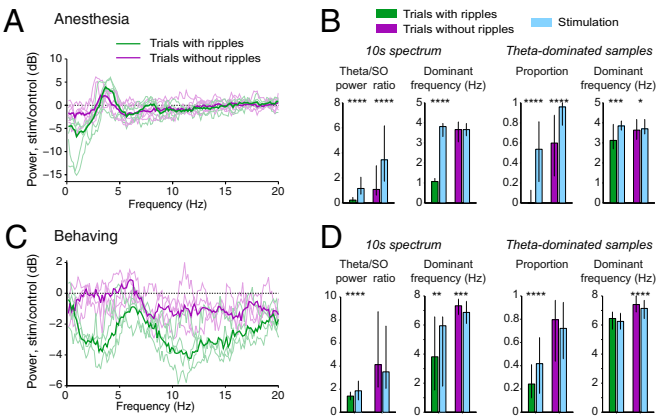

Fig. 5. Brain state dependence of MS stimulation effect. Recordings from anesthetized (*A* and *B*) and behaving (*C* and *D*) mice. (*A* and *C*) LFP power change in LM in ripple (green) versus theta (purple) trials. Thick lines: median of all trials; thin lines: individual animals. (*B* and *D*) Stimulation effect in each type of trials for (left to right) theta/slow oscillation ratio, spectral dominant frequency, proportion of theta-dominated samples, and median frequency of theta-dominated samples. **P* < 0.05, ***P* < 0.01, ****P* < 0.001, *****P* < 10^{-4}.

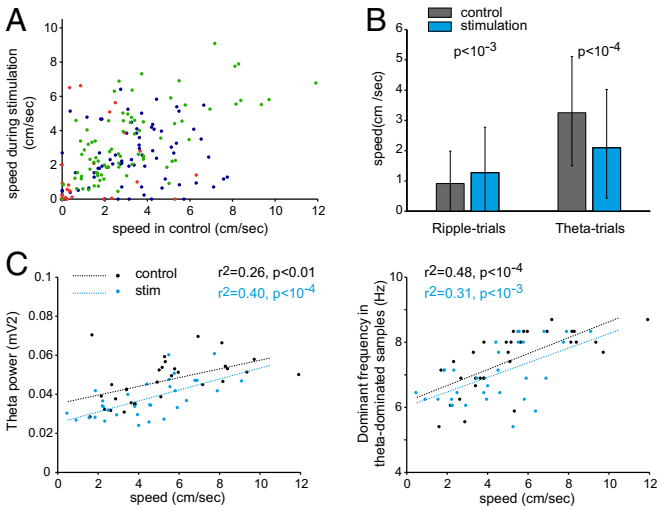

Fig. 6. Effect of MS stimulation on locomotor behavior. (*A*) Mean locomotion speed during control and stimulation epochs. Each dot is a single trial; colors: data for three individual mice. (*B*) Effect on mean locomotor speed during ripple trials (n = 90, three mice pooled) and theta-dominant trials (n = 129). (*C*) Correlation between speed and theta power (*Left*) or theta-dominant frequency (*Right*) in mouse 2, in control (black dots and line fit) and stimulation epochs (blue dots and line fit). Pearson's correlation coefficient and P values are indicated.

the release of glutamate from the presynaptic terminals of CA3 neurons (38, 39). In support of this hypothesis, adding the muscarinergic drug carbachol to the perfusion solution in in vitro investigation also abolishes spontaneously occurring SPW-Rs (16). Alternatively, or in addition, suppression of hippocampal axo-axonic neurons by transiently bursting septal GABAergic neurons may initiate SPW-Rs (40). This suggestion, however, leaves open the question of why a specific subset of septal inhibitory cells bursts during reduced cholinergic activity in the absence of theta oscillation. Overall, these findings can explain the competing, antagonistic relationship between SPW-Rs and theta oscillations (14).

Our results provide direct support for the role of ACh in enhancing theta oscillations (20) and the distinction between cholinergic-muscarinergic and noncholinergic mechanisms of theta oscillations (31). ChR-2–expressing cholinergic septal neurons faithfully followed the frequency of optogenetic stimulation, although frequency attenuation was obvious above 10 Hz. However, the frequency of induced LFP theta oscillations was independent of the entrainment frequency of septal cholinergic cells (Fig. 1). The lack of frequency-driving ability of cholinergic neurons is not surprising in light of the slow, second messenger-mediated mechanism of muscarinic receptors (41). Increasing the frequency of optogenetic stimulation simply increased theta power; this effect can be explained by the higher discharge rates of the septal cholinergic cells. Frequency control of theta oscillations, instead, may depend on the rhythmic firing patterns of septo-hippocampal GABAergic neurons (26, 28), which terminate exclusively on hippocampal inhibitory interneurons (42).

Another robust effect of optogenetic activation of MS cholinergic neurons in both anesthetized and behaving mice was the suppression of the power of slow oscillations (Fig. 3). These findings are similar to stimulation of basal forebrain cholinergic neurons, which reduced LFP power in the primary visual cortex in the 1- to 5-Hz band (43). One might argue that the reduction of hippocampal power in this band simply reflected changes in volume-conducted slow-frequency signals from the neocortex. However, previous work has demonstrated that slow oscillations also affect hippocampal circuits, as reflected by the entrained firing patterns (44, 45). Furthermore, MS cholinergic neurons do not project outside the limbic system (46), and thus their activation is not expected to exert a direct impact on neocortical activity. In addition to SPW-Rs and slow oscillations, optogenetic stimulation of the MS also suppressed power in the suprathetha frequency band. These observations parallel the competing effects between theta and suprathetha band activity because termination of theta-associated exploration in the intact animal is regularly coupled with enhanced "beta" power (47). The mechanisms of the suppressive effects of ACh on these oscillations are likely similar in the hippocampus and neocortex (43) and may be mediated, at least partially, by presynaptic M2 cholinergic receptor-mediated blockade of GABA release from basket and other interneurons (48).

Optogenetically induced activation of cholinergic neurons consistently increased low-frequency theta power and across-layer theta coherence in the anesthetized mouse, independent of whether stimulation occurred in the absence or presence of ongoing spontaneous theta activity (Figs. 3 and 4), as expected under the framework of the cholinergic model of theta generation (31, 49). A related interpretation of the differential effects of optogenetic stimulation of MS during anesthesia and waking is that the overall tone of ACh is lower under urethane than in the waking animal (50, 51). Thus, optogenetically assisted increase of cholinergic activity could increase ACh release effectively in the anesthetized mouse, as illustrated by the robust power changes in various frequency bands, but the same stimulation would exert fewer effects in the waking animal when levels of ACh are already high. The largest induced effect was observed in LM, a layer with a high density of cholinergic terminals (52) that were confirmed to be expressing ChR-2 in our immunostaining experiments. The same stimulation exerted a less clear effect on theta oscillations in the drug-free, behaving animal, because theta seen during movement is largely noncholinergically mediated, whereas the cholinergic input provides a background of sensory input-related drive to the hippocampus during movement. The effect of MS optogenetic drive was still observed by a significant increase of theta coherence between stratum Rad and LM below 7 Hz. These observations agree well with noncholinergic and cholinergic distinctions of theta oscillations related to motor and sensory integration, respectively (53). Overall, our findings provide perhaps the best example to date for a competition between cholinergic and noncholinergic types of theta rhythms during movement. They also demonstrate that the observed relationship between optogenetic stimulation of septal cholinergic cells and LFP power changes was not mediated by changes of motor behavior, because optogenetic stimulation of MS did not exert a consistent effect on locomotion speed, supporting previous observations (54).

Overall, cholinergic activation suppressed SPW-Rs entirely, strongly reduced the power of slow oscillations and suprathetha frequency oscillations, and increased theta power and coherence when the background activity contained little theta power. The relative enhancement of theta activity was thus largely due to the suppression of frequencies surrounding the theta band. In contrast, optogenetic activation brought about very little change in any frequency band when the background was characterized by high theta power. These results suggest that in the exploring and ambulating animal ACh release already maximally activates muscarinic receptors and, therefore, additional activation of septal cholinergic neurons has little impact.

Methods

Details on experimental procedures are provided in *Supporting Information*. Briefly, we used ChAT-Cre transgenic mice (n = 23) expressing ChR2 in their cholinergic neurons. The cre-dependent ChR2-containing construct was delivered to the MS either by viral gene transfer or by crossing the ChAT-Cre line with a ChR2-carrying floxed reporter line. ChAT-Cre mice injected with a control viral vector containing only the fluorescent reporter YFP were used as control for the effect of light (n = 3). Optical stimulation was achieved by transmitting light from a 473-nm laser source via an optic fiber to the MS. Both square pulse and sine wave stimulation were applied at frequencies from 0.5 to 20 Hz (pulse) or 0.5–12 Hz (sine). Multisite silicone probes were used for recording hippocampal local field potentials from several layers of the CA1-dentate axis in the dorsal hippocampus. LFP signal from all layers was spectrally decomposed and effect of stimulation on various frequency bands was determined before and after MS stimulation in both anesthetized and freely moving mice.

ACKNOWLEDGMENTS. We thank Győző Goda, Emőke Simon, Daniel English, Clémence Delarbre, Anne-Marie Godeheu, and Audrey Hay for assistance; Michaël Zugaro for comments on the manuscript; and Nikon Microscopy Center at the Institute of Experimental Medicine, Nikon Austria GmbH, and Auro-Science Consulting Ltd. for technical support. This work was supported by National Institutes of Health Grants NS-34994, MH-54671, and NS074015; National Science Foundation Grant 0542013; the J. D. McDonnell Foundation; European Union's Marie Curie Actions Grant FP7-PIOF-GA-2008-221834; European Union Framework Program 7 - European Research Council (EU-FP7-ERC)-2013 Starting Grant 337075; EU-FP7-ERC-2011 Advanced Grant 294313; Fondation pour la Recherche Médicale Grant SPE20061209127; Lendület program of the Hungarian Academy of Sciences and Human Frontiers Science Program Grant STF-000244/2009; Hungarian Scientific Research Fund Grant OTKA NF101773; and the National Brain Program of Hungary.

1. Harris KD, Thiele A (2011) Cortical state and attention. *Nat Rev Neurosci* 12(9):509–523.
2. Lee SH, Dan Y (2012) Neuromodulation of brain states. *Neuron* 76(1):209–222.
3. Jones BE (2005) From waking to sleeping: Neuronal and chemical substrates. *Trends Pharmacol Sci* 26(11):578–586.
4. Hasselmo ME, McGaughy J (2004) High acetylcholine levels set circuit dynamics for attention and encoding and low acetylcholine levels set dynamics for consolidation. *Prog Brain Res* 145:207–231.
5. Rasch B, Born J (2013) About sleep's role in memory. *Physiol Rev* 93(2):681–766.
6. Stumpf C, Petsche H, Gogolak G (1962) The significance of the rabbit's septum as a relay station between the midbrain and the hippocampus. II. The differential influence of drugs upon both the septal cell firing pattern and the hippocampus theta activity. *Electroencephalogr Clin Neurophysiol* 14:212–219.
7. Patil MM, Linster C, Lubenov E, Hasselmo ME (1998) Cholinergic agonist carbachol enables associative long-term potentiation in piriform cortex slices. *J Neurophysiol* 80(5):2467–2474.
8. Ovsepian SV, Anwyl R, Rowan MJ (2004) Endogenous acetylcholine lowers the threshold for long-term potentiation induction in the CA1 area through muscarinic receptor activation: in vivo study. *Eur J Neurosci* 20(5):1267–1275.
9. Leung LS, Shen B, Rajakumar N, Ma J (2003) Cholinergic activity enhances hippocampal long-term potentiation in CA1 during walking in rats. *J Neurosci* 23(28):9297–9304.
10. Buzsáki G (2002) Theta oscillations in the hippocampus. *Neuron* 33(3):325–340.
11. Parikh V, Kozak R, Martinez V, Sarter M (2007) Prefrontal acetylcholine release controls cue detection on multiple timescales. *Neuron* 56(1):141–154.
12. Marrosu F, et al. (1995) Microdialysis measurement of cortical and hippocampal acetylcholine release during sleep-wake cycle in freely moving cats. *Brain Res* 671(2):329–332.
13. Zhang H, Lin SC, Nicolelis MA (2010) Spatiotemporal coupling between hippocampal acetylcholine release and theta oscillations in vivo. *J Neurosci* 30(40):13431–13440.
14. Buzsáki G, Leung LW, Vanderwolf CH (1983) Cellular bases of hippocampal EEG in the behaving rat. *Brain Res* 287(2):139–171.
15. Norimoto H, Mizunuma M, Ishikawa D, Matsuki N, Ikegaya Y (2012) Muscarinic receptor activation disrupts hippocampal sharp wave-ripples. *Brain Res* 1461:1–9.
16. Zylla MM, Zhang X, Reichinnek S, Draguhn A, Both M (2013) Cholinergic plasticity of oscillating neuronal assemblies in mouse hippocampal slices. *PLoS ONE* 8(11):e80718.
17. Lawson VH, Bland BH (1993) The role of the septohippocampal pathway in the regulation of hippocampal field activity and behavior: Analysis by the intraseptal microinfusion of carbachol, atropine, and procaine. *Exp Neurol* 120(1):132–144.
18. Leutgeb S, Mizumori SJ (1999) Excitotoxic septal lesions result in spatial memory deficits and altered flexibility of hippocampal single-unit representations. *J Neurosci* 19(15):6661–6672.
19. Winson J (1978) Loss of hippocampal theta rhythm results in spatial memory deficit in the rat. *Science* 201(4351):160–163.
20. Lee MG, Chrobak JJ, Sik A, Wiley RG, Buzsáki G (1994) Hippocampal theta activity following selective lesion of the septal cholinergic system. *Neuroscience* 62(4):1033–1047.
21. Lubenov EV, Siapas AG (2009) Hippocampal theta oscillations are travelling waves. *Nature* 459(7246):534–539.
22. Patel J, Fujisawa S, Berényi A, Royer S, Buzsáki G (2012) Traveling theta waves along the entire septotemporal axis of the hippocampus. *Neuron* 75(3):410–417.
23. Wang XJ (2002) Pacemaker neurons for the theta rhythm and their synchronization in the septohippocampal reciprocal loop. *J Neurophysiol* 87(2):889–900.
24. Geisler C, et al. (2010) Temporal delays among place cells determine the frequency of population theta oscillations in the hippocampus. *Proc Natl Acad Sci USA* 107(17):7957–7962.
25. Huh CY, Goutagny R, Williams S (2010) Glutamatergic neurons of the mouse medial septum and diagonal band of Broca synaptically drive hippocampal pyramidal cells: Relevance for hippocampal theta rhythm. *J Neurosci* 30(47):15951–15961.
26. Hangya B, Borhegyi Z, Szilágyi N, Freund TF, Varga V (2009) GABAergic neurons of the medial septum lead the hippocampal network during theta activity. *J Neurosci* 29(25):8094–8102.
27. Dragoi G, Carpi D, Recce M, Csicsvari J, Buzsáki G (1999) Interactions between hippocampus and medial septum during sharp waves and theta oscillation in the behaving rat. *J Neurosci* 19(14):6191–6199.
28. Simon AP, Poindessous-Jazat F, Dutar P, Epelbaum J, Bassant MH (2006) Firing properties of anatomically identified neurons in the medial septum of anesthetized and unanesthetized restrained rats. *J Neurosci* 26(35):9038–9046.
29. Zhang H, Lin SC, Nicolelis MA (2011) A distinctive subpopulation of medial septal slow-firing neurons promote hippocampal activation and theta oscillations. *J Neurophysiol* 106(5):2749–2763.
30. Tóth K, Borhegyi Z, Freund TF (1993) Postsynaptic targets of GABAergic hippocampal neurons in the medial septum-diagonal band of broca complex. *J Neurosci* 13(9):3712–3724.
31. Kramis R, Vanderwolf CH, Bland BH (1975) Two types of hippocampal rhythmical slow activity in both the rabbit and the rat: Relations to behavior and effects of atropine, diethyl ether, urethane, and pentobarbital. *Exp Neurol* 49(1 Pt 1):58–85.
32. Newman EL, Gillet SN, Climer JR, Hasselmo ME (2013) Cholinergic blockade reduces theta-gamma phase amplitude coupling and speed modulation of theta frequency consistent with behavioral effects on encoding. *J Neurosci* 33(50):19635–19646.
33. Buzsáki G, Czopf J, Kondákor I, Kellényi L (1986) Laminar distribution of hippocampal rhythmic slow activity (RSA) in the behaving rat: Current-source density analysis, effects of urethane and atropine. *Brain Res* 365(1):125–137.
34. Royer S, et al. (2010) Multi-array silicon probes with integrated optical fibers: Light-assisted perturbation and recording of local neural circuits in the behaving animal. *Eur J Neurosci* 31(12):2279–2291.
35. Soltesz I, Deschênes M (1993) Low- and high-frequency membrane potential oscillations during theta activity in CA1 and CA3 pyramidal neurons of the rat hippocampus under ketamine-xylazine anesthesia. *J Neurophysiol* 70(1):97–116.
36. Colom LV, Ford RD, Bland BH (1987) Hippocampal formation neurons code the level of activation of the cholinergic septohippocampal pathway. *Brain Res* 410(1):12–20.
37. Ylinen A, et al. (1995) Sharp wave-associated high-frequency oscillation (200 Hz) in the intact hippocampus: Network and intracellular mechanisms. *J Neurosci* 15(1 Pt 1):30–46.
38. Fernández de Sevilla D, Cabezas C, de Prada AN, Sánchez-Jiménez A, Buño W (2002) Selective muscarinic regulation of functional glutamatergic Schaffer collateral synapses in rat CA1 pyramidal neurons. *J Physiol* 545(Pt 1):51–63.
39. Hasselmo ME, Schnell E (1994) Laminar selectivity of the cholinergic suppression of synaptic transmission in rat hippocampal region CA1: Computational modeling and brain slice physiology. *J Neurosci* 14(6):3898–3914.
40. Viney TJ, et al. (2013) Network state-dependent inhibition of identified hippocampal CA3 axo-axonic cells in vivo. *Nat Neurosci* 16(12):1802–1811.
41. Eglen RM (2012) Overview of muscarinic receptor subtypes. *Handbook Exp Pharmacol* 208(208):3–28.
42. Freund TF, Antal M (1988) GABA-containing neurons in the septum control inhibitory interneurons in the hippocampus. *Nature* 336(6195):170–173.
43. Pinto L, et al. (2013) Fast modulation of visual perception by basal forebrain cholinergic neurons. *Nat Neurosci* 16(12):1857–1863.
44. Wolansky T, Clement EA, Peters SR, Palczak MA, Dickson CT (2006) Hippocampal slow oscillation: a novel EEG state and its coordination with ongoing neocortical activity. *J Neurosci* 26(23):6213–6229.
45. Isomura Y, et al. (2006) Integration and segregation of activity in entorhinal-hippocampal subregions by neocortical slow oscillations. *Neuron* 52(5):871–882.
46. Gaykema RP, Luiten PG, Nyakas C, Traber J (1990) Cortical projection patterns of the medial septum-diagonal band complex. *J Comp Neurol* 293(1):103–124.
47. Quinn LK, Nitz DA, Chiba AA (2010) Learning-dependent dynamics of beta-frequency oscillations in the basal forebrain of rats. *Eur J Neurosci* 32(9):1507–1515.
48. Gulyás AI, et al. (2010) Parvalbumin-containing fast-spiking basket cells generate the field potential oscillations induced by cholinergic receptor activation in the hippocampus. *J Neurosci* 30(45):15134–15145.
49. Lawrence JJ (2008) Cholinergic control of GABA release: Emerging parallels between neocortex and hippocampus. *Trends Neurosci* 31(7):317–327.
50. Materi LM, Semba K (2001) Inhibition of synaptically evoked cortical acetylcholine release by intracortical glutamate: involvement of GABAergic neurons. *Eur J Neurosci* 14(1):38–46.
51. Clement EA, et al. (2008) Cyclic and sleep-like spontaneous alternations of brain state under urethane anesthesia. *PLoS ONE* 3:e2004.
52. Frotscher M, Léránth C (1985) Cholinergic innervation of the rat hippocampus as revealed by choline acetyltransferase immunocytochemistry: A combined light and electron microscopic study. *J Comp Neurol* 239(2):237–246.
53. Bland BH (2008) Anatomical, physiological, and pharmacological properties underlying hippocampal sensorimotor integration. *Information Processing by Neuronal Populations*, eds Hölscher C, Munk M (Cambridge Univ Press, Cambridge, UK), pp 283–325.
54. Bland BH, Bird J, Jackson J, Natsume K (2006) Medial septal modulation of the ascending brainstem hippocampal synchronizing pathways in the freely moving rat. *Hippocampus* 16(1):11–19.